Synthesis, Antitumor Activities and Molecular Modelling of 4-Anilinoquinazoline Derivatives as EGFR-TK Inhibitors

Rania M. Gomaa
Mansoura University Faculty of Pharmacy
Magda A. El-Sayed
Mansoura University Faculty of Pharmacy
Khalid Bashir Selim (khbselim2000@yahoo.com)
Mansoura University, Faculty of Pharmacy https://orcid.org/0000-0001-9255-6847

Research Article

Keywords: 4-Anilino-6-quinazoline, EGFR, Erlotinib, Kinase inhibition, Cytotoxicity, Apoptosis

Posted Date: January 14th, 2022

DOI: https://doi.org/10.21203/rs.3.rs-1222057/v1

Abstract

New compounds of 4-anilino-6-substituted quinazoline were designed, synthesized and tested for their EGFR-TK and tumor growth inhibitory activities. The synthesized compounds were appended with amides **6** and **7**, dithiocarbamate ester **8a–f** or urea/thiourea **9–12** moieties at C-6 of the quinazoline ring to work as extra hydrogen bond acceptors. All the synthesized compounds were effective against EGFR-TK activity, particularly, derivatives **8a**, **8f** and **9** with IC_{50} values of 0.14±0.003, 0.119±0.003, and 0.115±0.002 μM, respectively, showed the best activities. The three compounds were further assayed for their cytotoxicity against MCF-7, H-69, SKOV-3 and LS-174T cell lines. Multikinase enzymes inhibition activity of compound **9** was further screened including VEGFR-2, c-MER, c-MET and Her-2. Compounds **8a**, **8f**, and **9** were docked into the ATP binding site of EGFR-TK which also had resemblance binding pattern to erlotinib with extra binding mode with Cys-773 at the gatekeeper of the enzyme. Cell cycle analyses of MCF-7 cells treated with **8a** and **9** was measured in addition to other related factors such as Bax, Bcl-2, caspase-9, and PARP-1.

Introduction

Cancer is continuing to be a major health problem in developing and developed countries [1]. WHO reported in 2020, that the incidence of population is 18.1 million cancer cases and mortality about 9.6 million deaths occurred [2]. It is regarded as the second leading cause of mortality, after cardiovascular diseases. Among women, breast cancer has stood out as the most frequently diagnosed cancer as well as the second largest cause of cancer-related deaths in women [3].

Epidermal Growth Factor Receptor (EGFR) consists of a family of four different tyrosine kinases (TKs) including EGFR (HER1), HER2, HER3 and HER4 that plays a critical role in the development of multiple cellular functions including cell growth, survival, propagation, differentiation and cell death. EGFR consists of an extracellular, a transmembrane, and an intracellular tyrosine kinase domain [4]. Upon binding of the ligands to the extracellular domain, dimerization occurs with other receptors triggering autophosphorylation of tyrosine residues with the catalytic domain thus activating downstream cell signaling pathways and subsequent signal transduction [4, 5]. There are two ways to inhibit EGFR either by blocking ligand binding to the extracellular domain with monoclonal antibodies or by small-molecule inhibitors which interact with the ATP-binding region [6].

Based on the understanding of the competitive binding to the ATP catalytic active site, the first generation was 4-anilinoquinazoline-based derivatives such as Erlotinib (Tarceva®) [7] and gefitinib (Iressa®) [8] which are reversible competitors of ATP for binding with the tyrosine kinase. Lapatinib is a reversible dual inhibitor of EGFR and HER2 and is approved for the breast cancer therapy. [9]. Dacomitinib is highly selective second-generation small-molecule inhibitor of EGFR, HER2 and HER4, that specifically and irreversibly binds to and inhibits these receptors, resulting in inhibition of proliferation and induction of apoptosis in EGFR-expressing tumor cells [10], also Afatinib (Gilotrif®) [11] is an example for the second generation, which is irreversibly bound to EGFR-TKIs (Fig. 1).

In 4-anilinoquinazoline-based EGFR inhibitors, the essential parts required for the inhibition are shown in Figure 2. N-1 atom of the quinazoline ring binds with the backbone NH of Met769, in the ATP-binding pocket, *via* hydrogen bonding. Similarly, a water (HOH-10) molecule-induced hydrogen bonding interaction is noticed between the N-3 atom of the quinazoline ring and Thr766 side chain [4, 6, 12]. The aniline ring completely occupies the adjacent hydrophobic region of the EGFR kinase domain and the free NH linker of aniline is clearly optimal [6]. Electron-withdrawing lipophilic substituents on the 3-position of the aniline are favorable and only very small groups are preferred, while the substitution of the aniline side chain with larger groups will significantly reduce activity as limited bulk tolerance [13]. In some studies new compounds demonstrated that compounds having Br atom at position 3 of the anilino moiety showed better activity than Cl atom at the same position [14]. On the other side of the quinazoline scaffold, introducing electron-donating group with polar properties was favorable at C-6 and/or C-7 positions which lays adjacent to the hydrophilic region to improve the physicochemical properties and to provide a better pharmacokinetic feature [6]. The introduction of large groups at the 5- and 8- positions is not desirable for high potency, because larger groups at these two positions may introduce unfavorable *van der Waals* interaction with EGFR [15].

In this research, two series of novel 6-substituted-4-anilinoquinazolines were designed to specifically inhibit EGFR. The first series contains amide/dithiocarbamate moieties **6**–**8** and the second series contains urea/thiourea moieties **9**–**12**, both at C-6 of the quinazoline scaffold. By this way, these new polar solubilizing moieties could target the hydrophilic regions of the protein kinase domain's ATP-binding site to develop different selectivity for the designed molecules and to improve their inhibitory effects by improving their physicochemical properties. The synthesized anilinoquinazolines were assessed for their inhibitory ability towards EGFR enzyme and MCF-7, H-69, SKOV-3 and LS-174T cancer cell lines expressing EGFR. Also, flexible docking program such as MOE was used to expect the binding affinity and orientation of the target compounds **8a**, **8f** and **9** at the active region of the EGFR-TK ATP binding site. Furthermore, flow cytometry was also used to evaluate their effect on the cell cycle of MCF-7 cells.

Experimental

General

All chemicals and solvents were ordered from the Aldrich-Sigma and alpha company which were utilized with no more purification. Using precoated aluminum sheet silica gel MERCK 60 F245 (TLC technique), the reactions progressed and the spots formed were seen using a UV lamp (366 nm). Dichloromethane/methanol (10:1), petroleum ether/ethyl acetate (1:1) and (1:3) were used as elution solvents. ^{1}H and ^{13}C NMR spectra were obtained using JEOL 500 MHz spectrometer and Bruker Avance III HD FT high resolution 400 MHz spectrometer at Faculty of Pharmacy's Unit of NMR, respectively, Mansoura University and TMS was used as an internal standard and chemical shifts were indicated as ppm and coupling constants (*J*) were reported in Hz. Mass spectrometry (APCI, or APCI/ASAP) m/z analyses were performed Advion compact mass spectrometer (CMS) NY |USA.

Synthesis of N4-(3-bromophenyl)quinazoline-4,6-diamine (4)

*N*4-(3-bromophenyl)quinazoline-4,6-diamine (**4**) was prepared in accordance with the procedure described in the papers [6,10,17,18] 2-amino-5-Nitroanthranilonitrile **1** (0.95 gm, 5.9 mmol, 1.0 eq) was suspended in dimethylformamide dimethyl acetal (4 mL) and the mixture was refluxed for 2 hr. After cooling to room temperature, the mixture was refrigerated for 24 hours. The resulting yellow precipitate was filtered, washed with ethyl ether, and dried to yield **3** (Yield 92%). A mixture of **2** (0.99 gm, 4.516 mmol, 1.0 eq) and 3-bromoaniline (1.1 eq) were heated and stirred at reflux in acetic acid (5 mL) for 2 hr. Aniline and acetic acid would be mixed together in the reaction flask first, followed by the addition of **2** within one min. This procedure is used to prevent lumps from forming between them. The yellow precipitate that obtained was filtered hot, washed with water, diethyl ether and dried to provide the required nitroquinazoline **3** (Yield 90%). To a mixture of 6-nitroquinazoline **3** (1 mmol), Pd/C and MeOH (7 mL) was added $NH_2NH_2{\cdot}H_2O$ (2 mL), and the obtained solution was heated at 80 °C reflux condition for 30 min. Then the mixture was filtered and concentrated in vacuo. The crude material was washed with water and filtered.

General procedure for preparation N-{4-((3-bromophenyl) amino) quinazolin-6-yl}-2-chloro/bromoacetamide (5)

A solution of *N*-4-(3-bromophenyl)quinazoline-4,6-diamine (**4**) (0.2 gm, 0.635 mmol, 1 eq) dissolved in 5 mL dichloromethane was added to a cooled solution of chloroacetyl chloride (0.698 mmol, 1.1 eq) dissolved in 5 mL dichloromethane and then added pyridine (1.27 mmol, 2 eq) then stirred for 2 hr in ice bath. The reaction mixture was evaporated under reduced pressure only without heating to form a green precipitate which used in the following step with no more purification.

General procedure for preparation of compounds 6 and 7

A solution of cyclic secondary amine (0.615 mmol, 1 eq) in DMF (3 mL) was stirred with *N*-{4-((3-bromophenyl)amino)quinazolin-6-yl}-2-chloro acetamide (**5**) (1eq) then added K_2CO_3 (1.23 mmol, 2 eq) at room temperature for 24 hr. The reaction mixture was spilled over ice to produce a precipitate that could then be filtered, washed with water and recrystallized by petroleum ether to afford the titled compounds.

N-{4-((3-bromophenyl)amino)quinazolin-6-yl}-2-(4-phenylpiperazin-1-yl)acetamide (6)

Brown solid, Yield = 60%, M.P = 102-104 °C. IR (KBr, υ, cm^{-1}): 3447 (NH), 3286 (NH), 1686 (C=O), 1601 (C=N), 528 (C-Br); ^{1}H NMR (400 MHz, DMSO-d_6), δ (ppm): 2.7 (s, 4H, $2CH_2$), 3.22 (s, 4H, $2CH_2$), 3.26 (s, 2H, CH_2), 6.76 (dd, *J* = 7.1, 7.1 Hz, 1H, ArH), 6.94 (d, *J* = 8.1 Hz, 2H, ArH), 7.10 (dd, J = 7.3, 7.2 Hz, 1H, ArH), 7.18 (dd, *J* = 7.7, 7.6 Hz, 2H, ArH), 7.35 (dd, *J* = 7.7, 7.6 Hz, 2H, ArH), 7.88-7.71 (m, 2H, ArH), 8.03 (d, *J* = 8.5 Hz, 1H, ArH), 8.49 (s, 1H, ArH), 8.62 (s, 1H, pyrim-H), 9.76 (s, 1H, NH; D_2O exchangeable H), 10.02 (s, 1H, NHCO; D_2O exchangeable H); ^{13}C NMR (100 MHz, DMSO-d_6), δ (ppm): 48.59, 53.27, 62.05, 101.23, 112.89, 115.79, 115.92, 119.36, 122.25, 123.04, 124.19, 127.7, 128.7, 128.92, 129.44, 136.63, 139.67,

147.07, 151.45, 153.39, 158.0, 169.1; APCI-MS (m/z): 517 (M^+); Elemental analysis for $C_{26}H_{25}BrN_6O$, calcd.: C, 60.35; H, 4.87; N, 16.24. Found: C, 60.24; H, 4.86; N, 16.27.

N-{4-((3-bromophenyl)amino)quinazolin-6-yl}-2-(4-(pyrimidin-2-yl)piperazin-1-yl)acetamide (7)

Dark green solid, yield = 70%, M.P =107-109 °C. IR (KBr, υ, cm^{-1}): 3423 (NH), 3337 (NH), 1670 (C=O), 1586 (C=N), 527 (C-Br); ^{1}H NMR (400 MHz, DMSO-d_6), δ (ppm): 2.62 (s, 4H, $2CH_2$), 3.26 (s, 2H, CH_2), 3.82 (s, 4H, $2CH_2$), 6.62 (dd, *J* = 4.6, 4.6 Hz, 1H, ArH), 7.28 (d, *J* = 8.4 Hz, 1H, ArH), 7.32 (d, *J* = 7.6 Hz, 1H, ArH), 7.78 (d, *J* = 9.0 Hz, 1H, ArH), 7.85 (d, *J* = 8.1 Hz, 1H, ArH), 8.02 (d, *J* = 9.2 Hz, 1H, ArH), 8.16 (s, 1H, ArH), 8.35 (d, *J* = 4.7 Hz, 2H, ArH), 8.57 (s, 1H, ArH), 8.66 (s, 1H, pyrim-H), 9.88 (s, 1H, NH), 10.09 (s, 1H, NHCO); ^{13}C NMR (100 MHz, DMSO-d_6), δ (ppm): 43.58, 52.99, 62.02, 103.27, 110.65, 112.83, 121.37, 121.62, 123.03, 124.79, 125.85, 126.40, 128.03, 128.89, 130.83, 136.86, 141.68, 153.61, 157.75, 158.44, 161.69; Elemental analysis for $C_{24}H_{23}BrN_8O$, calcd.: C, 55.5; H, 4.46; N, 21.57. Found: C, 55.39; H, 4.45; N, 21.61.

General procedure for preparation of compounds (8a-8f)

A solution of cyclic secondary amine (0.615 mmol, 1 eq) in DMF (3 mL) and CS_2 (3.077 mmol, 5 eq) was stirred 5 min. then added a finely divided powder of $Na_3PO_4.H_2O$ (0.615 mmol, 1 eq) and stirred at room temperature for 4 hr. Then added to intermediate *N*-{4-((3-bromophenyl)amino)quinazolin-6-yl}-2-chloroacetamide (**5**) and the mixture was stirred at room temperature until the reaction was complete, then poured into ice to obtain a precipitate that was filtered, washed with water and recrystallized with petroleum ether.

2-{[4-((3-bromophenyl)amino)quinazolin-6-yl]amino}-2-oxoethy piperidine-1-carbodithioate (8a)

Green solid, yield = 55%, M.P = 180-182 °C. IR (KBr, υ, cm^{-1}): 3339 (NH), 3224 (NH), 1696 (C=O), 1611 (C=N), 1226 (C=S), 533 (C-Br); ^{1}H NMR (500 MHz, DMSO-d_6), δ (ppm): 1.58 (s, 4H, $2CH_2$), 1.67 (d, *J* = 4.8 Hz, 2H, CH_2), 3.95 (s, 2H,CH_2), 4.21 (s, 2H,CH_2), 4.35 (s, 2H, CH_2S), 7.28 (d, *J* = 8.1 Hz, 1H, ArH), 7.34 (dd, *J* = 8.1, 8.0 Hz, 1H, ArH), 7.79 (d, *J* = 9.0 Hz, 1H, ArH), 7.88-7.81(m, 2H, ArH), 8.14 (d, *J* = 1.7 Hz, 1H, ArH), 8.57 (s, 1H, ArH), 8.72 (d, *J* = 1.7 Hz, 1H, pyrim-H), 9.95 (s, 1H, NH), 10.64 (s, 1H, NHCO); ^{13}C NMR (100 MHz, DMSO-d_6), δ (ppm): 23.95, 25.68, 26.31, 41.60, 51.18, 51.66, 112.2, 116.0, 120.6, 121.4, 123.1, 124.8, 126.4, 128.86, 130.84, 137.19, 141.60, 147.09, 153.79, 157.69, 166.3, 193.4; Elemental analysis for $C_{22}H_{22}BrN_5OS_2$, calcd.: C, 51.16; H, 4.29; N, 13.56; S, 12.42. Found: C, 51.27; H, 4.28; N, 13.54; S, 12.44.

2-{[4-((3-bromophenyl)amino)quinazolin-6-yl]amino}-2-oxoethyl morpholine-4-carbodithioate (8b)

Green solid, yield = 40%, M.P = 95-97 °C. IR (KBr, υ, cm^{-1}): 3447 (NH), 3347 (NH), 1679 (C=O), 1598 (C=N), 1231 (C=S), 538 (C-Br); ^{1}H NMR (500 MHz, DMSO-d_6), δ (ppm): 3.69-3.65 (m, 4H, $2CH_2$), 3.97 (s, 2H, CH_2), 4.20 (s, 2H, CH_2), 4.37 (s, 2H, CH_2S), 7.27 (dd, *J* = 7.5, 1.8 Hz, 1H, ArH), 7.38-7.30 (m, 1H, ArH), 7.78 (d, *J* = 8.9, 1H, ArH), 7.89-7.81 (m, 2H, ArH), 8.13 (dd, *J* = 1.9, 1.8 Hz, 1H, ArH), 8.56 (s, 1H, ArH), 8.71

(d, *J* = 1.8 Hz, 1H, pyrim-H), 9.94 (s, 1H, NH), 10.64 (s, 1H, NHCO); Elemental analysis for $C_{21}H_{20}BrN_5O_2S_2$, calcd.: C, 48.65; H, 3.89; N, 13.51; S, 12.37. Found: C, 48.68; H, 3.88; N, 13.53; S, 12.39.

2-{[4-((3-bromophenyl)amino)quinazolin-6-yl]amino}-2-oxoethyl 4-propylpiperazine-1-carbodithioate (8c)

Brown solid, yield = 30%, M.P = 119-121 °C. IR (KBr, υ, cm^{-1}): 3449 (NH), 3384 (NH), 1701 (C=O), 1601 (C=N), 1268 (C=S), 517 (C-Br); ^{1}H NMR (400 MHz, DMSO-d_6), δ (ppm): 0.84 (t, *J* = 7.1 Hz, 3H, CH_3), 1.47-1.35 (m, 2H, CH_2), 2.31-2.22 (m, 2H, CH_2), 3.47 (s, 4H, $2CH_2$), 3.93 (s, 2H, CH_2), 4.16 (s, 2H, CH_2), 4.33 (s, 2H, CH_2S), 7.55-7.23 (m, 2H, ArH), 7.91-7.60 (m, 3H, ArH), 8.12 (d, *J* = 3.1Hz, 1H, ArH), 8.54 (s, 1H, ArH), 8.69 (s, 1H, pyrim-H), 9.92 (s, 1H, NH), 10.62 (s, 1H, NHCO); APCI-MS (m/z): 560.8 (M^+); Elemental analysis for $C_{24}H_{27}BrN_6OS_2$, calcd.: C, 51.52; H, 4.86; N, 15.02; S, 11.46. Found: C, 51.49; H, 4.87; N, 15.05; S, 11.44.

2-{[4-((3-bromophenyl)amino)quinazolin-6-yl]amino}-2-oxoethyl 4-cyclohexylpiperazine-1-carbodithioate (8d)

Buff solid, yield = 30%, M.P = 109-111 °C. IR (KBr, υ, cm^{-1}): 3491(NH), 3360 (NH), 1679 (C=O), 1600 (C=N), 1232 (C=S), 527 (C-Br); ^{1}H NMR (400 MHz, DMSO-d_6), δ (ppm): 1.18-1.07 (m, 4H, $2CH_2$), 1.20 (s, 1H,CH), 1.54 (d, *J* = 11.2 Hz, 1H, CH), 1.70 (d, *J* = 8.3 Hz, 4H, $2CH_2$), 2.30–2.22 (m, 1H, CH), 2.56 (s, 4H, $2CH_2$), 3.91 (s, 2H, CH_2), 4.16 (s, 2H, CH_2), 4.33 (s, 2H, CH_2S), 7.30-7.24 (m, 2H, ArH), 7.78-7.73 (m, 1H, ArH), 7.89-7.80 (m, 2H, ArH), 8.13 (s, 1H, ArH), 8.55 (s, 1H, ArH), 8.71 (s, 1H, pyrim-H), 9.93 (s, 1H, NH), 10.63 (s, 1H, NHCO); Elemental analysis for $C_{27}H_{31}BrN_6OS_2$, calcd.: C, 54.08; H, 5.21; N, 14.02; S, 10.7. Found: C, 54.03; H, 5.20; N, 14.05; S, 10.68.

2-{[4-((3-bromophenyl)amino)quinazolin-6-yl]amino}-2-oxoethyl 4-phenylpiperazine-1-carbodithioate (8e)

Yellowish Brown solid, yield = 60%, M.P = 128-130 °C. IR (KBr, υ, cm^{-1}): 3490 (NH), 3355 (NH), 1677 (C=O), 1601 (C=N), 1221 (C=S), 525 (C-Br); ^{1}H NMR (400 MHz, DMSO-d_6), δ (ppm): 4.12 (s, 4H, $2CH_2$), 4.34 (s, 4H, $2CH_2$), 4.37 (s, 2H, CH_2S), 6.79 (dd, *J* = 7.3, 7.1 Hz, 1H, ArH), 6.94 (d, *J* = 8.1 Hz, 2H, ArH), 7.22 (dd, *J* = 7.9, 7.7 Hz, 3H, ArH), 7.32 (dd, *J* = 8, 7.8 1H, ArH), 7.87-7.72 (m, 3H, ArH), 8.12 (s, 1H, ArH), 8.55 (s, 1H, ArH), 8.71 (s, 1H, pyrim-H), 9.95 (s, 1H, NH), 10.65 (s, 1H, NHCO); ^{13}C NMR (100 MHZ, DMSO-d_6), δ (ppm): 31.19, 36.27, 48.09, 112.13, 115.97, 119.80, 121.45, 121.59, 124.86, 126.34, 128.86, 128.98, 129.56, 130.79, 133.75, 135.47, 136.57, 137.27, 141.60, 141.90, 149.50, 150.50, 153.52, 162.80, 195.00; Elemental analysis for $C_{27}H_{25}BrN_6OS_2$, calcd.: C, 54.63; H, 4.25; N, 14.16; S, 10.8. Found: C, 54.59; H, 4.26; N, 14.19; S, 10.82.

2-{(4-((3-bromophenyl)amino)quinazolin-6-yl)amino}-2-oxoethyl 4-(pyrimidin-2-yl)piperazine-1-carbodithioate (8f)

Pale Green solid, yield = 75%, M.p = 190-192 °C. IR (KBr, υ, cm^{-1}): 3447 (NH), 3317 (NH), 1689 (C=O), 1582 (C=N), 1228 (C=S), 525 (C-Br); ^{1}H NMR (400 MHz, DMSO-d_6), δ (ppm): 3.87 (s, 4H, $2CH_2$), 4.12 (d, *J* =

6.9 Hz, 2H, CH_2), 4.34 (s, 2H, CH_2), 4.38 (s, 2H, CH_2S), 6.68 (dd, *J* = 4.5, 4.2 Hz, 1H, ArH), 7.43-7.09 (m, 3H, ArH), 7.92-7.73 (m, 3H, ArH), 8.13 (s, 1H, ArH), 8.39 (d, *J* = 4.3 Hz, 1H, ArH), 8.63-8.48 (m, 1H, ArH), 8.71 (s, 1H, pyrim-H), 10.01 (s, 1H, NH), 10.66 (s, 1H, NHCO); ^{13}C NMR (100 MHz, DMSO-d_6), δ (ppm): 34.89, 43.95, 44.01, 111.15, 113.0, 121.28, 121.57, 123.2, 125.0, 125.28, 126.59, 127.8, 128.6, 128.76, 128.9, 130.87, 138.84, 148.47, 158.44, 165.47, 172.76, 195.0; APCI-MS (m/z): 597.1 ($M+H^+$); Elemental analysis for $C_{25}H_{23}BrN_8OS_2$, calcd.: C, 50.42; H, 3.89; N, 18.82; S, 10.77. Found: C, 50.47; H, 3.88; N, 18.79; S, 10.75.

General procedure for preparation of compounds (9-12)

A solution of *N*4-(3-bromophenyl)quinazoline-4,6-diamine (**4**) (0.1 gm, 0.317 mmol, 1 eq) in pyridine (3 mL) was reacted with adequate isocyanate or iso(thio)cyanate (0.317 mmol, 1 eq) stirred for 6 hr at room temperature. The reaction mixture was poured into cold dil. HCl and the formed precipitate was filtered, washed with water, dried and recrystallized by diethyl ether.

1-{4-((3-bromophenyl)amino)quinazolin-6-yl}-3-(4-nitrophenyl)urea (9)

Olive green, yield = 80%, M.P = 294-296 °C. ^{1}H NMR (400 MHz, DMSO-d_6), δ (ppm): 7.27-7.07 (m, 3H, ArH), 7.38 (d, *J* = 8.8 Hz, 2H, ArH), 7.43 (d, *J* = 8.7 Hz, 1H), 7.68-7.58 (m, 1H), 7.81 (d, *J* = 8.9 Hz, 1H, ArH), 7.89 (dd, *J* = 8.4, 8.3 Hz, 2H, ArH), 8.52-8.40 (m, 1H, ArH), 8.59 (s, 1H, pyrim-H), 9.99 (s, 1H, NH; D_2O exchangeable H), 10.33 (s, 1H, NH; D_2O exchangeable H), 11.35 (s, 1H, NH; D_2O exchangeable H); Elemental analysis for $C_{21}H_{15}BrN_6O_3$, calcd.: C, 52.63; H, 3.15; N, 17.53. Found: C, 52.67; H, 3.16; N, 17.56.

1-{4-((3-bromophenyl)amino)quinazolin-6-yl}-3-(p-tolyl)urea (10)

Green solid, yield = 85%, M.P = 241-243 °C. IR (KBr, υ, cm^{-1}): 3470 (NH), 3324 (NH), 2919 (C-H), 1713 (C=O), 1613 (C=N), 536 (C-Br); ^{1}H NMR (400 MHz, DMSO-d_6), δ (ppm): 2.07 (s, 3H, CH_3), 6.89 (d, *J* = 8.3 Hz, 1H, ArH), 6.95 (d, *J* = 8.2 Hz, 2H, ArH), 7.17 (dd, *J* = 8.8, 8.4 Hz, 1H, ArH), 7.24 (d, *J* = 8.3 Hz, 2H, ArH), 7.38-7.29 (m, 2H, ArH), 7.49 (d, *J* = 8.0 Hz, 1H, ArH), 7.72 (d, *J* = 9.0 Hz, 1H, ArH), 7.92 (d, *J* = 9.0 Hz, 1H, ArH), 8.66 (s, 1H, pyrim-H), 9.23 (s, 1H, NH; D_2O exchangeable H), 9.57 (s, 1H, NH; D_2O exchangeable H), 11.43 (s, 1H, NH; D_2O exchangeable H); Elemental analysis for $C_{22}H_{18}BrN_5O$, calcd.: C, 58.94; H, 4.05; N, 15.62. Found: C, 59.01; H, 4.04; N, 15.65.

1-{4-((3-bromophenyl)amino)quinazolin-6-yl}-3-(4-methoxyphenyl)thiourea (11)

Yellowish green, yield = 80%, M.P = 184-186 °C. IR (KBr, υ, cm^{-1}): 587 (C-Br), 1242 (C=S), 1614 (C=N), 2960 (C-H), 3425 (NH), 3285 (NH); ^{1}H NMR (400 MHz, DMSO-d_6), δ (ppm): 3.71 (s, 3H), 6.89 (d, *J* = 8.6 Hz, 2H, ArH), 7.35 (d, *J* = 8.5 Hz, 2H), 7.48-7.39 (m, 2H, ArH), 7.69 (dd, *J* = 8.2, 7.3 Hz, 1H), 7.84 (d, *J* = 8.9 Hz, 1H, ArH), 8.02 (s, 1H,ArH), 8.12 (d, *J* = 8.4 Hz, 1H, ArH), 8.65 (s, 1H, ArH), 8.86 (s, 1H, ArH, pyrim-H), 10.33 (s, 1H, NH; D_2O exchangeable H), 10.37 (s, 1H, NH; D_2O exchangeable H), 11.15 (s, 1H, NH; D_2O exchangeable H); ^{13}C NMR (100 MHz, DMSO-d_6), δ (ppm): 55.7, 114.2, 114.4, 118.7, 121.4, 121.7, 123.6, 125.16, 126.3, 127.2, 129.3, 131.17, 132.4, 134.8, 139.3, 140.2, 151.1, 157.18, 159.6, 180.95; Elemental

analysis for $C_{22}H_{18}BrN_5OS$, calcd.: C, 55.01; H, 3.78; N, 14.58; S, 6.67. Found: C, 54.94; H, 3.77; N, 14.61; S, 6.68.

1-{4-((3-bromophenyl)amino)quinazolin-6-yl{-3-(naphthalen-2-yl)urea (12)

Olive green solid, yield = 83%, M.P = 285-287 °C. IR (KBr, υ, cm^{-1}): 3338 (NH), 3267 (NH), 1722 (C=O), 1627 (C=N), 533 (C-Br); ^{1}H NMR (400 MHz, DMSO-d_6), δ (ppm): 7.50-7.40 (m, 3H, ArH), 7.57-7.51 (m, 2H, ArH), 7.60 (d, *J* = 6.7 Hz, 1H), 7.65 (d, *J* = 8.4 Hz, 1H, ArH), 7.70 (d, *J* = 7.7 Hz, 1H, ArH), 7.95-7.87 (m, 1H, ArH), 7.98 (d, *J* = 1.5, 1H, ArH), 8.04 (d, *J* = 7.4 Hz, 1H, ArH), 8.09 (d, *J* = 8.8 Hz, 1H, ArH), 8.30 (dd, *J* = 8.4, 8.2 Hz, 1H, ArH), 8.90-8.64 (m, 2H, ArH), 9.41 (s, 1H, NH; D_2O exchangeable H), 10.26 (s, 1H, NH; D_2O exchangeable H), 11.38 (s, 1H, NH; D_2O exchangeable H); ^{13}C NMR (100 MHz, DMSO-d_6), δ (ppm): 110.64, 114.89, 117.85, 121.6, 122.4, 123.2, 124.38, 125.64, 126.12, 126.26, 126.4, 127.1, 127.98, 128.8, 129.2, 131.1, 134.2, 134.6, 135.1, 139.1, 140.99, 143.9, 153.5, 154.0, 160.0; APCI-MS (m/z): 484.1 ($M+H^+$); Elemental analysis for $C_{25}H_{18}BrN_5O$, calcd.: C, 61.99; H, 3.75; N, 14.46. Found: C, 62.11; H, 3.76; N, 14.43.

Biological assays

Enzyme inhibition assay

EGFR inhibition assay

The EGFR kinase assay kit was used to test the newly synthesized compounds for their ability to inhibit EGFR, which was applied in a proper 96-well format and contains a sufficient amount of pure recombinant EGFR enzyme, EGFR substrate, ATP and kinase assay buffer for 100 enzyme reactions. Erlotinib was chosen as the reference EGFR inhibitor.

Add 20 µL of diluted EGFR enzyme to the wells labelled "Positive Control" and "Test Inhibitor Control" to start the reaction. Incubate for 40 min at 30 °C. Thaw Kinase-Glo Max reagent. Add 50 µL of Kinase-Glo Max reagent to every well after the 40 min reaction. Cover the plate with aluminum foil and incubate the plate at room temperature for 15 min then measure the luminescence with the microplate reader.

VEGFR-2 inhibition assay

VEGFR-2 kinase activity was measured using the detection reagent Kinase-Glo® MAX. 96-well plates with purified recombinant VEGFR-2 enzyme, VGFR-2 substrate, ATP and kinase assay buffer were applied to the VEGFR-2 kinase Assay kit. After preparing the positive control, test inhibitor and blank wells, diluted VEGFR-2 enzyme was incorporated into the positive control and also into the test inhibitor, followed by 40 min of incubation at 30 °C. Then, each well was loaded with Kinase-Glo® MAX reagent and incubated for 45 min at room temperature. Cover the plate with aluminum foil and incubate the plate at room temperature for 15 min, then use the microplate reader to measure the luminescence.

c-MER inhibition assay

The c-MER Kinase Assay kit uses ADP-Glo® as a detection reagent to measure c-MER activity for screening and profiling applications. The c-MER Kinase Assay Kit comes in a convenient 96-well format, with enough purified recombinant c-Mer enzyme, c-MER substrate peptide, ATP and kinase assay buffer for 100 enzyme reactions using erlotinib as standard.

Initiate the reaction by adding 10 µL of diluted c-MER enzyme into the “Positive Control” and "Test Inhibitor Control" wells. Incubate at 30 °C for 45 min. Then thaw the ADP-Glo reagent. After the 45 min reaction, add 25 µL of ADP-Glo reagent to every well and incubate the plate at room temperature for 45 min. Add 50 µm of kinase-Detection reagent. Cover the plate with aluminum foil and incubate it at room temperature for another 45 min. The microplate reader is used to measure luminescence. A “Blank” value is subtracted from all readings.

c-MET inhibition assay

The c-MET Exon 14 Del Kinase Assay Kit is designed to measure c-MET exon 14 deletion kinase activity utilizing Kinase-Glo® MAX as a detection reagent added to 96-well plates and erlotinib as a standard for screening and profiling applications. The c-MET Exon Del 14 Kinase Assay Kit comes in a proper 96-well format, with a sufficient amount of pure recombinant c-MET Exon 14 Del enzyme, c-MET substrate, ATP and kinase assay buffer for 100 enzyme reactions. Initiate the reaction by adding 20 µL of diluted c-MET Exon 14 del enzyme to the wells labelled “Positive Control” and "Test Inhibitor Control". Incubate at 30 °C for 45 min. Thaw Kinase-Glo Max reagent. Add 50 µL of Kinase-Glo Max reagent to each well after 45 min of the reaction. Cover the plate with aluminum foil and incubate the plate for 15 min at room temperature. Immediately read the sample in a luminometer or microtiter-plate capable of reading luminescence. A “Blank” value is subtracted from all readings.

Her-2 inhibition assay

The Her-2 Kinase Assay Kit uses Kinase-Glo® MAX as a detection reagent to detect Her-2 kinase activity for screening and profiling applications. Purified recombinant Her-2 enzyme, Her-2 substrate, ATP and kinase assay buffer were applied to 96-well plates with Her-2 kinase test kit. After preparing the positive control, test inhibitor and blank wells, diluted Her-2 enzyme was added to both the positive control and test inhibitor, followed by 40 min incubation at 30°C. The Kinase-Glo® MAX reagent was then applied to each well and incubated for 45 min at room temperature. Cover the plate with aluminum foil and incubate the plate at room temperature for 15 min, then use the microplate reader to measure luminescence.

Cytotoxicity evaluation using a viability assay

The cytotoxic activity was assessed using the 3-(4,5-dimethylthiazol-2-yl)-2,5-diphenyl tetrazolium bromide (MTT) colorimetric assay in four tumor cell lines namely; ovarian carcinoma cell line (SKOV-3), Lung carcinoma cell line (H-69), Breast carcinoma cell line (MCF-7) and Colon carcinoma cell line (LS-174T) .

Reassemble each vial of MTT (M-5655) to be used with 3 mL of medium or balanced salt solution without phenol red and serum after removing cultures from the incubator into a laminar flow hood or other sterile work area. 10% of the culture medium volume was added to reconstitute MTT. Return the cultures to the incubator for 2-4 hr depending on the type of cell and the highest density of cells. A 2 hr incubation period is usually sufficient, while it can be extended for low cell densities or cells with lower metabolic activity. When doing comparisons, incubation times have to be similar. Remove the cultures from the incubator once the incubation period has ended and dissolve the formazan crystals by applying the same volume of MTT Solubilization solution (M-8910) as the original culture medium. Pipetting up and down [trituration] may be required to completely dissolve the MTT formazan crystals in some cases, particularly in dense cultures. Finally, at a wavelength of 570 nm, the spectrophotometer was measured. At 690 nm, measure the background absorbance of multiwell plates and subtract it from the 570 nm reading.

Cell cycle analysis and apoptosis detection

Flow cytometry was used to scan the cell cycle analysis and investigate apoptosis. The Annexin V Apoptosis Detection Kit is based on the observation that soon after initiating apoptosis, cells translocate the membrane phosphatidylserine (PS) from the inner face of the plasma membrane to the cell surface. Once on the cell surface, PS can be easily detected by staining with a fluorescent conjugate of Annexin V, a protein that has a high affinity for PS. Induce apoptosis by the desired method. 1-5 x 10^5 cells was collected by centrifugation and resuspended in 500 µL of 1X Binding Buffer. Add 5 µL of Annexin V-FITC and 5 µL of propidium iodide (PI 50 mg/mL). Incubate at room temperature for 5 min in the dark. Analyze Annexin V-FITC binding by flow cytometry using a FITC signal detector (usually FL1) and PI staining by the phycoerythrin emission signal detector.

Measurement of the effect of compounds 8a and 9 on the levels of Bax and Bcl-2

Bax assay

Except the human Bax-α standard, all reagents should be kept at room temperature for at least 30 min before use. All standards, controls and samples should be tested twice. Determine the number of wells to be utilized using the Assay Layout Sheet, then insert any remaining wells with the desiccant back into the pouch and close the ziploc. Pipette 100 µL of each sample into the appropriate wells and keep the rest of the wells at 4 °C. Tap the plate gently to mix the contents. Seal the plate and incubate at room temperature on a plate shaker for 1 hour at ~500 rpm, then empty the contents of the wells and wash each one with 400 µL of wash solution. For a total of 5 rinses, do the wash 4 more times and empty or aspirate the wells after the final wash, then firmly tap the plate on a lint-free paper towel to eliminate any residual wash buffer.

Put 100 µL of yellow antibody into each well, except the blank one. Seal the plate and incubate at room temperature for 1 hour at ~500 rpm on a plate shaker. Evacuate the contents of the wells and wash each one with 400 µL of wash solution. For a total of 5 rinses, repeat the wash 4 more times. Fill or aspirate the

wells after the last wash, then firmly tap the plate on a lint-free paper towel to eliminate any residual wash buffer. Add 100 µL of blue Conjugate to each well, except the Blank. Close the plate and incubate at room temperature for 30 min at ~500 rpm on a plate shaker. Drain the contents of the wells and wash each one by adding 400 µL of wash solution. For a total of 5 rinses, repeat the wash four more times. Fill or aspirate the wells after the last wash, then firmly tap the plate on a lint-free paper towel to eliminate any residual wash buffer. Pipet 100 µL of substrate solution into each well and on a plate shaker adjusted to 500 rpm, incubate for 30 min at room temperature. Pipet 100 µL stop solution to each well and detect the optical density at 450 nm, usually with a correction between 570 and 590 nm, with the plate reader set towards the blank wells.

If the plate reader cannot be blanked against the blank wells, calculate the result by subtracting the mean optical density of the blank wells from all the readings.

Bcl-2 assay

Wash the microwells twice with approximately 300 µL of wash buffer per well with thorough aspiration of microwell contents between washes. After washing, empty the wells and tap the microwell strips on an absorbent pad or paper towel to drain the remaining wash buffer. Utilize the microwell strips right away once they've been washed, or leave them upside down on damp absorbent paper for no more than 15 min.

To all standard wells and to the blank wells, add 100 µL of sample diluent in duplicate. Prepare doubles of the standard (1:2 dilution) with concentrations ranging from 32 ng/mL to 0.5 ng/mL. Add 100, 80, 20 µL respectively, of sample diluent, in duplicate, to the blank wells. To all wells, having the blank wells, add 50 µL of diluted biotin-conjugate. Cover with a plate cover and incubate at room temperature, on a microplate shaker at 100 rpm if available, for 2 hours. Add 100 µL of diluted Streptavidin-HRP to all wells, including the blank wells. Cover with a plate cover and incubate at room temperature, on a microplate shaker at 100 rpm if available, for 1 hour. Pipette 100 µL of mixed TMB Substrate Solution into all wells, including the blanks. Incubate the microwell strips at room temperature (18 to 25 °C) for about 15 min, if available on a rotator set at 100 rpm. Avoid direct exposure to intense light. The point, at which the substrate reaction is stopped, is often determined by the ELISA reader. Many ELISA readers record absorbance only up to 2.0 O.D. Therefore the color development within individual microwells must be watched by the person running the assay and the substrate reaction stopped before positive wells are no longer properly detectable. Stop the enzyme reaction by quickly pipetting 100 µL of stop solution into each well, including the blank wells. It is important that the stop solution is spread quickly and uniformly throughout the microwells to completely inactivate the enzyme. If the microwell strips are stored at 2–8 °C in the dark, results must be read spontaneously after the stop solution is introduced, or within one hour. Read absorbance of each microwell using a spectrophotometer with a using primary wave length 450 nm (optionally 620 nm as the reference wave length; 610 nm to 650 nm) is valid and calculate the result.

Caspases-9 assay

For cell lysis, follow the cell lysate protocol. Determine the number of microwell strips required to test the desired number of samples plus the appropriate number of wells needed for running blanks and standards. Each sample, standard, blank and optional control sample should be assayed in duplicate. In duplicate, pour 100 µL of sample diluent into the blank wells. Fill the sample wells with 50 µL of Sample Diluent. Add 50 µL of each sample in duplicate to the sample wells. Add 50 µL of detection monoclonal antibody to human caspase-9 antibody to all wells. Incubate at room temperature (18 °C to 25 °C) for 2 hours, at 200 rpm, and then add 100 µL of diluted anti-rabbit-IgG-HRP to all wells, and also for the blank wells. Incubate at room temperature (18 °C to 25 °C) for 1 hour, at 200 rpm and proceed immediately to the next step. 100 µL of TMB Substrate Solution should be pipetted to all wells.

Incubate the microwell strips at room temperature (18 °C to 25 °C) for about 10 min. The color development on the plate should be monitored and the substrate reaction stopped before positive wells are no longer properly recordable. Alternatively, the color development can be monitored by the ELISA reader at 620 nm. Read the absorbance of every microwell on a spectrophotometer using 450 nm as the primary wave length (optionally 620 nm as the reference wave length; 610 nm to 650 nm is valid). Blank the plate reader according to the manufacturer's instructions with the use of the blank wells. Determine the absorbance of both the samples and the standards and calculate the result.

PARP-1 Assay

Equilibrate all reagents and materials to ambient room temperature prior to use in the procedure. Optimal results for intra- and inter-assay reproducibility will be obtained when performing incubation steps at 37°C as indicated below. Detect the required number of wells and return any residual unused wells and desiccant to the pouch. Add 100 µL of serially titrated standards, diluted samples or blank into the wells of the PARP1 Microplate. At least two replicates of each standard, sample or blank is recommended. Cover the plate with the well plate lid and incubate at 37°C for 2 hours. Remove the plate lid and discard the liquid in the wells by rigorously flicking it into an acceptable waste receptacle or aspiration. Gently blot any remaining liquid from the wells by tapping inverted on the benchtop onto paper toweling. Do not allow the wells to completely dry out at any time. Add 100 µL of prepared 1X Biotinylated PARP1 detector antibody to each well. Cover with the well-plate lid and incubate at 37°C for 60 min and discard the liquid in the wells by rigorously flicking it into an acceptable waste receptacle or aspiration. Gently blot any remaining liquid from the wells by tapping inverted on the benchtop onto paper toweling. Do not allow the wells to completely dry out at any time. Wash the plate 3 times with 1X wash buffer then add 100 µL of prepared 1X Avidin-HRP Conjugate into each well and incubate at 37°C for 60 min. Discard the liquid in the wells by rigorously flicking it into an acceptable waste receptacle or aspiration. Gently blot any remaining liquid from the wells by tapping inverted on the benchtop onto paper toweling. Do not allow the wells to completely dry out at any time. Wash the plate 5 times with 1X Wash Buffer as in Step 10.10. Add 90 µL of TMB Substrate to each well and incubate at 37°C in the dark for 15-30 min. Wells should change to gradations of blue. If the color is too deep, reduce the incubation time. Add 50 µL of stop solution to each well. Well color should change to yellow immediately. Add the stop solution in the same well order as done for the TMB Substrate. Read the O.D. absorbance at 450 nm with a standard

microplate reader within 5 min of stopping the reaction in step 10.16. If wavelength correction is available, set it to 540 nm or 570 nm and calculate the result.

Molecular docking

MOE was used for all molecular modelling calculations and docking investigations. The most active analogs of EGFR inhibitors (**8a**, **9f** and **9**) docked against Erlotinib as a ligand compound. Energy minimization and multiple conformers studied along the active site of the EGFR ATP binding site (PDB ID: 1m17) to compare the structural similarities of our analogues to Erlotinib, which has a higher binding affinity with a lower energy profile ranging from -8.3437 to -7.1982 kcal/mol in comparison to Erlotinib -7.9161 kcal/mol and showed the best overlay with lead compound. In terms of hydrogen bonding with the Met769 and Thr766 with the quinazoline ring, they had the same binding affinity to the receptor of concern.

Results And Discussion

Chemistry

In this study, the method for obtaining the desired quinazolines is illustrated in Schemes 1–3. The key intermediate 6-amino-4-anilinoquinazoline (**4**) [6, 16] was prepared according to the reported procedure (Scheme 1) *via* reaction of **1** and DMF-DMA to afford *N*-(2-cyano-4-nitrophenyl)-*N*,*N*-dimethylformimidamide (**2**) [17]. The nitro quinazoline **3** [6, 10] was obtained through cyclization of compound **2** with 3-bromoaniline in glacial acetic acid, which then reduced using Pd and NH_2NH_2 in methanol [18] to yield the corresponding amine **4**.

Schemes 1 and 2 show the preparation of series 1 through acylation of compound **4** with chloroacetyl chloride under basic condition to give chloro derivative **5** which was reacted either with substituted piperazines to give amides **6** and **7** or with the adequate cyclic secondary amine (morpholine and piperidine) or four piperazines and carbon disulfide in DMF and $Na_3PO_4{\cdot}H_2O$ to afford dithiocarbamate derivatives **8a**–**f**. While, Scheme 3 shows the synthesis of series 2 including (thio) urea derivatives **9**–**12** by substituting the amino compound **4** with the adequate iso(thio)cyanates in pyridine. The newly synthesized compounds' spectroscopic results (^{1}H and ^{13}C-NMR) agree with the predicted structures as detailed in the experimental part.

Biological activity

Measurement of potential EGFR inhibitory activity (IC_{50})

Table 1 IC_{50} of EGFR-TK inhibitory activity for compounds **6**, **7** and **8a**–**f**

Compound No.	Results of inhibition of EGFR Tyrosine Kinase (IC_{50} μM)
6	0.44±0.01
7	0.28±0.01
8a	0.14±0.003
8b	0.18±0.004
8c	0.17±0.004
8d	0.46±0.01
8e	0.20±0.004
8f	0.119±0.003
Erlotinib	0.138±0.003

As shown in Table 1, amides **6** and **7** and dithiocarbamate ester **8a**–**f** were evaluated for their inhibitory activities towards EGFR enzymatic assay. The majority of the compounds showed high inhibition in micro molar range (IC_{50} from 0.119 to 0.46 μM) using Erlotinib as a reference of (IC_{50} = 0.138±0.003 μM). The structural modification of dithiocarbamte derivatives and their EGFR inhibitory action were studied and showed that compounds **8a**, **8b** and **8c** having heterocyclic rings piperidine, morpholine and *N*-propyl piperazine, respectively, are the most potent when compared to other substituted piperazines which carry *N*-cyclohexyl and *N*-phenyl moieties. Interestingly, the *N*-pyrimidinyl piperazine derivative in **8f** proved to be the most potent EGFR inhibitor (IC_{50} = 0.119±0.003 μM) among this series. This may give an indication that the polarity is important for the enzyme inhibition particularly when compared to compounds **8d** and **8e** which contain non polar moieties with IC_{50} values equal to 0.47±0.01 and 0.2±0.004, respectively. To clarify the importance of dithiocarbamte moiety, additional two compounds **6** and **7** were synthesized and the results shows that the absence of dithiocarbamte moiety reduces the inhibitory activity of both compounds with IC_{50} values equal to 0.44±0.01 μM and 0.28±0.01 μM, respectively, toward EGFR enzyme (entries **8e** and **8f** *versus* entries **6** and **7**, respectively).

Table 2 IC_{50} of EGFR-Tk inhibitory activity for compounds **9**–**12**

Compound No.	Results of inhibition of EGFR Tyrosine Kinase (IC_{50} μM)
9	0.115±0.002
10	0.250±0.005
11	0.160±0.003
12	0.240±0.005
Erlotinib	0.138±0.003

On the other hand, the urea and thiourea derivatives of series 2 were evaluated for their EGFR inhibitory activity (Table 2). The results showed that phenyl urea derivative **12** has the half potency (IC_{50} = 0.24±0.005 μM) when compared to erlotinib as a reference (IC_{50} = 0.138±0.003 μM). The activity was enhanced to be equal to erlotinib by inserting the polar nitro group at para position of the phenyl moiety **9**. The non-polar methyl group at para position diminishes the activity to the half (IC_{50} = 0.25±0.005 μM), while the activity was retained when replacing the non-polar para methyl group in the urea compound **10** with the polar para methoxy group in the thiourea compound **11** (IC_{50} = 0.16±0.003 μM).

In vitro cytotoxic activity

Table 3 Cytotoxic activity (IC_{50}) of compounds **8a**, **8f**, and **9** against four cell lines

Compound No.	Cytotoxicity (IC_{50} μM)				Enzyme inhibition (IC_{50} μM)
	MCF-7	H-69	SKOV-3	LS-174T	EGFR
8a	7.27±0.4	19.77±1.1	12.9±0.7	15.11±0.8	0.140±0.003
8f	70.14±3.8	162.9±8.8	54.97±3.0	12.5±0.7	0.119±0.003
9	16.55±0.9	6.057±0.3	24.94±1.4	54.53±3.4	0.115±0.002
Erlotinib	3.89±0.2	17.51±0.9	5.21±0.3	15.5±1.22	0.138±0.003

The most potent EGFR inhibitors **8a**, **8f**, and **9** were tested against four cancer cell lines, which are over-expressing EGFR enzyme, such as breast cancer (MCF-7) [19], small cell lung cancer (H-69) [20], human ovarian cancer (SKOV-3) [21], and human colon cancer (LS-174T) [22,23] utilizing the 3-(4,5-dimethylthiazol-2-yl)-2,5-diphenyl tetrazolium bromide (MTT) colorimetric test [24] (Table 3). Among the three tested compounds, dithiocarbamate **8a** shows broad spectrum against the four cells with the highest cytotoxic activity with IC_{50} ranging from 7.27±0.4 to 19.77±1.1 when compared to the reference drug. Compound **8f** was the least active member towards the four cell lines except LS-174T (IC_{50} = 12.5±0.7). While, compound **9** exhibits the highest activity against H-69 cell line (IC_{50} = 6.057±0.3) and better than the reference drug (IC_{50} = 17.51±0.9).

Multi-kinases inhibition assay

Table 4 Multi-kinases inhibitory activity for compound **9**

Compound No.	Enzyme inhibition (IC_{50} μM)			
	Her-2	c-MER	c-MET	VEGFR-2
9	0.05±0.003	0.045±0.003	0.04±0.002	0.11±0.006
Erlotinib	0.04±0.002	0.09±0.005	0.06±0.004	0.07±0.004

As depicted in Table 4, compound **9** was chosen for additional multi-kinases inhibition assay *versus* vascular endothelial growth factor (VEGFR-2), human epidermal growth factor receptor 2 (HER-2), c-mesenchymal-epithelial transition factor (c-MET) and mer tyrosine kinase (c-MER), which showed the highest inhibitory activity than erlotinib against EGFR enzymes and H-69 cancer cells,. Compound **9** exhibited excellent inhibitory activity against c-MER and c-MET with IC_{50} values of 0.045±0.003 µM and 0.04±0.002 µM, respectively, better than the reference drug erlotinib. Also, it exhibited high activity against HER-2 and VEGFR-2 with IC_{50} values of 0.05±0.003 µM and 0.11±0.006 µM, respectively.

Apoptosis assay

Apoptosis is one of the techniques used to assess the success of cancer treatments [25]. In MCF-7 cells, flow cytometry was used to determine the apoptotic activity of compounds **8a** and **9** using propidium iodide (PI) staining and annexin-V-FITC [26]. The studied compound **8a** produced an increase in late apoptosis from 0.23 % to 19.4 %, as well as an increase in early apoptosis from 0.36 % to 4.04 %, with necrosis percent 13.59 % *versus* 0.82 % in the control MCF-7 cell (Fig. 3). For compound **9**, there was a rise in the late apoptosis from 0.23% to 11.84% and a rise in the early apoptosis from 0.36% to 2.35% with necrosis percent 7.15% *versus* 0.82% produced by the control MCF-7 cell **(**Fig. 3), whereas the reference drug erlotinib has an increase in the late apoptosis from 0.23% to 19.74% and an increase in the early apoptosis from 0.36% to 3.67% with necrosis percent 11.51% *versus* 0.82% produced by the control MCF-7 cell. It was shown that the late apoptosis percentage induced by **8a** and **9** were higher than that of the early phase, implying that the apoptotic cells could be recovered to safe ones. The data collected indicated that compounds **8a** and **9** inhibit cancer cell proliferation through apoptosis.

Cell cycle arrest

Compounds **8a** and **9** were further assayed of their actions towards cell cycle progression at the following checkpoints G1 (start), S (metaphase), and G2/M [27] in MCF-7 cells against Erlotinib for 24 hr using propidium iodide (PI) and flow cytometer (FCM) for analysis [28]. According to the data obtained, it showed that there were cell accumulations of 37.03% and 7.26% at pre G1 and G2/M phases in MCF-7 cells treated with **8a** and 21.52% and 5.87% with **9**, respectively, in compared to the untreated cells (1.41% and 9.63%) (Table 5). On the other hand, G0/G1 population was 46.51% and 57.12% after treatment with compounds **8a** and **9**, respectively, when compared to the controlled cells 55.42%. The results of the cell cycle analysis is consistent with the data obtained from the apoptosis assay indicate that compounds **8a** and **9** are apoptotic inducers.

Table 5 Results of cell cycle analysis of compounds **8a** and **9** in MCF7

Compound No.	Cell cycle analysis (%)			
	G0-G1	S	G2/M	Pre-G1
8a	46.51	46.23	7.26	37.03
9	57.12	37.01	5.87	21.52
Erlotenib	62.02	29.77	8.21	34.92
Control	55.42	34.95	9.63	1.41

The effect of compounds 8a and 9 on Bax and Bcl-2

Bax and Bcl-2 are main mitochondrial factors which involve in the control of the cell apoptosis [29]. So, the effects of **8a** and **9** on the apoptotic factors Bax and Bcl-2 were examined in this study. Compounds **8a** and **9** were incubated in the MCF-7 cancer cells for 24 hr at its IC_{50}; 7.27 and 16.55 µM, respectively. In compared to untreated cells, the investigated drugs **8a**, **9** and erlotinib enhanced the levels of Bax proteins by 10, 9 and 13 folds, respectively (Table 6). While compounds **8a**, **9** and erlotinib enhanced the levels of Bcl-2 proteins approximately by half compared to the untreated cells (Table 6).

Table 6 The effect of compounds **8a** and **9** on Bax, Bcl-2, Casp-9 and PARP-1 against erlotinib in MCF-7 cells

Compound No.	Bax	Bcl-2	Casp-9	PARP-1
	pg/ mL		ng/ mL	
8a	403±6.17	2.822±0.12	23.43±1.7	5.673±0.27
9	362.4±6.09	4.708±0.20	19.99±0.72	8.742±0.34
Erlotinib	499.5±9.79	3.527±0.13	25.15±1.4	5.813±0.29
Control	40.14±2.88	8.72±0.26	3.42±0.26	14.06±1.29

Upregulation of caspase-9 and PARP-1 Cleavage Assay

For further illustrating the apoptotic effects of compound **8a** and **9**, we assessed the appropriate expression pattern of protein using In vitrogen EIA kit human Caspase 9 as shown in Table 6. Expression of caspase-9 increased upon treatment with the tested compounds from 3.42±0.26 to 23.43±1.7 ng/ mL for **8a** and from 3.42±0.26 to 19.99±0.72 ng/ mL for **9**. In addition, poly (ADP-ribose) polymerase 1 (PARP-1) is an abundant and ubiquitous nuclear enzyme. When active, it captures NAD^+ to assemble long and branching molecules of poly (ADP-ribose) (pADPr), thereby modifying itself and surrounding nuclear proteins that PARP-1 binds the promoters of genes involved in the determination of cell self-identity and carcinogenesis [30]. The obtained results showed that **8a**, **9** and erlotinib reduced the level of PARP-1 enzyme, approximately to the half, when compared to the untreated cells (Table 6).

Molecular docking

The interaction among the tested compounds and the EGFR enzyme's ATP pocket was investigated utilizing a computational molecular docking analysis using MOE [31]. The most potent inhibitors **8a**, **8f**, and **9** were used as ligands in this research, with the structure of EGFR as the docking model (PDB ID: 1m17) and erlotinib's reported binding form in the X-ray crystal structure of the EGFR kinase active site (Fig. 5). The results indicate that compound **8a** and **8f** form two H-bonding between Met769 and Thr766 by the formation of H-bonding between the N1 and N3 of the quinazoline ring, respectively, as an illustration of dithiocarbamate derivatives. Hydrophobic region binds with Lys721 and carbon disulfide linkage to form new bond with EGFR which explains the importance of the presence of the dithiocarbamte moiety (Fig. 5). While, compound **9** as an illustration of urea derivatives strongly linked to the key amino acid Met769 and Thr766 by the formation of H-bonding between the N1 and N3, respectively, and the polar NO_2 group to form covalent bond with Ser696 (Fig. 5). Also, the lead compound, erlotinib, was docked in the active site of EGFR kinase (PDB ID: 1m17), which was shown to obtain the reported binding mode of erlotinib in the 3D structure of the active site of EGFR kinase (Fig. 5), where the N1 atom of quinazoline binds *via* H-bond with the backbone NH of Met769.

The designed compounds **8a**, **8f** and **9** have higher binding affinity with a lower energy range between -8.3437 to -7.1982 kcal/mol, compared to Erlotinib -7.9161 kcal/mol. the average distance between atoms of the new pose selected and the original ligand rmsd_refine 1.9719, 1.2455 and 1.7604, respectively, with a similar binding to the receptor of interest sharing the hydrogen bonding towards Met793 and Thr766 the quinazoline moiety showed with better overlay (Fig. 6).

Conclusion

Two new series of 4-anilino-6-substituted-quinazolines with (thio)urea or dithiocarbamate linkers were synthesized and their antitumor activity against EGFR inhibition was investigated *in vitro*. Among the tested compounds, **8a** and **8f** (with dithiocarbamate group) and **9** (with urea group) were the most potent inhibitors against EGFR in comparison to erlotinib as a reference drug. Those three compounds tested against four cell lines MCF-7, H-69, SKOV-3 and LS-174T, where **8a** shows the highest cytotoxic activity, among the three tested compounds, **8f** exhibits the highest activity against LS-174T and **9** exhibits the highest activity against H-69 cell line. Moreover, compound **9** exhibited high multi-inhibitory activities against extra kinases such as VEGFR-2, HER2, c-MET and c-MER. Also, the induction of apoptosis for **8a** and **9** and their effect on cell cycle phases in MCF-7 cells were tested.

References

1. El-Azab AS, Al-Omar MA, Abdel-Aziz AA, Abdel-Aziz NI, el-Sayed MA, Aleisa AM et al (2010) Design, synthesis and biological evaluation of novel quinazoline derivatives as potential antitumor agents: molecular docking study. Eur J Med Chem 45:4188–4198
2. Rezki N, Almehmadi MA, Ihmaid S, Shehata AM, Omar AM, Ahmed HEA et al (2020) Novel scaffold hopping of potent benzothiazole and isatin analogues linked to 1,2,3-triazole fragment that mimic

quinazoline epidermal growth factor receptor inhibitors: Synthesis, antitumor and mechanistic analyses. Bioorg Chem 103:104133

3. Abdelsalam EA, Zaghary WA, Amin KM, Abou Taleb NA, Mekawey AAI, Eldehna WM et al (2019) Synthesis and in vitro anticancer evaluation of some fused indazoles, quinazolines and quinolines as potential EGFR inhibitors. Bioorg Chem 89:102985
4. George RF, Kandeel M, El-Ansary DY, El Kerdawy AM (2020) Some 1,3,5-trisubstituted pyrazoline derivatives targeting breast cancer: Design, synthesis, cytotoxic activity, EGFR inhibition and molecular docking. Bioorg Chem 99:103780
5. Ghorab MM, Alsaid MS, Soliman AM, Dual (2018) EGFR/HER2 inhibitors and apoptosis inducers: New benzo[g]quinazoline derivatives bearing benzenesulfonamide as anticancer and radiosensitizers. Bioorg Chem 80:611–620
6. Mowafy S, Farag NA, Abouzid KA (2013) Design, synthesis and in vitro anti-proliferative activity of 4,6-quinazolinediamines as potent EGFR-TK inhibitors. Eur J Med Chem 61:132–145
7. Perez-Soler R (2004) The role of erlotinib (Tarceva, OSI 774) in the treatment of non-small cell lung cancer. Clin Cancer Res 10:4238s–42340shttps://doi.org/10.1158/1078-0432.CCR-040017.
8. Hanke JH, Hughes LR (2004) Targeted therapies for cancer – from tamoxifen to gefitinib ('Iressa'). Drug Discovery Today: Therapeutic Strategies 1:411–416
9. Burris HA 3, Hurwitz HI, Dees EC, Dowlati A, Blackwell KL, O'Neil B et al (2005) Phase I safety, pharmacokinetics, and clinical activity study of lapatinib (GW572016), a reversible dual inhibitor of epidermal growth factor receptor tyrosine kinases, in heavily pretreated patients with metastatic carcinomas. J Clin Oncol 23:5305–5313
10. Cavalieri S, Perrone F, Miceli R, Ascierto PA, Locati LD, Bergamini C et al (2018) Efficacy and safety of single-agent pan-human epidermal growth factor receptor (HER) inhibitor dacomitinib in locally advanced unresectable or metastatic skin squamous cell cancer. Eur J Cancer 97:7–15
11. Miller VA, Hirsh V, Cadranel J, Chen Y-M, Park K, Kim S-W et al (2012) Afatinib versus placebo for patients with advanced, metastatic non-small-cell lung cancer after failure of erlotinib, gefitinib, or both, and one or two lines of chemotherapy (LUX-Lung 1): a phase 2b/3 randomised trial. Lancet Oncol 13:528–538
12. Stamos J, Sliwkowski MX, Eigenbrot C (2002) Structure of the epidermal growth factor receptor kinase domain alone and in complex with a 4-anilinoquinazoline inhibitor. J Biol Chem 277:46265–46272
13. Rewcastle GW, Denny WA, Bridges AJ, Zhou H, Cody DR, McMichael A et al (1995) Tyrosine kinase inhibitors. 5. Synthesis and structure-activity relationships for 4-[(phenylmethyl)amino]- and 4-(phenylamino)quinazolines as potent adenosine 5'-triphosphate binding site inhibitors of the tyrosine kinase domain of the epidermal growth factor receptor. J Med Chem 38:3482–3487
14. Li HQ, Li DD, Lu X, Xu YY, Zhu HL (2012) Design and synthesis of 4,6-substituted-(diaphenylamino)quinazolines as potent EGFR inhibitors with antitumor activity. Bioorg Med Chem 20:317–323

15. Hou T, Zhu L, Chen L, Xu X (2003) Mapping the binding site of a large set of quinazoline type EGF-R inhibitors using molecular field analyses and molecular docking studies. J Chem Inf Comput Sci 43:273–287. https://doi.org/10.1021/ci025552a
16. Ismail RSM, Abou-Seri SM, Eldehna WM, Ismail NSM, Elgazwi SM, Ghabbour HA et al (2018) Novel series of 6-(2-substitutedacetamido)-4-anilinoquinazolines as EGFR-ERK signal transduction inhibitors in MCF-7 breast cancer cells. Eur J Med Chem 155:782–796
17. Elkamhawy A, Farag AK, Viswanath AN, Bedair TM, Leem DG, Lee KT et al (2015) Targeting EGFR/HER2 tyrosine kinases with a new potent series of 6-substituted 4-anilinoquinazoline hybrids: Design, synthesis, kinase assay, cell-based assay, and molecular docking. Bioorg Med Chem Lett 25:5147–5154
18. Zeidan MA, Mostafa AS, Gomaa RM, Abou-Zeid LA, El-Mesery M, El-Sayed MA et al (2019) Design, synthesis and docking study of novel picolinamide derivatives as anticancer agents and VEGFR-2 inhibitors. Eur J Med Chem 168:315–329
19. Park K, Han S, Shin E, Kim HJ, Kim JY (2007) EGFR gene and protein expression in breast cancers. Eur J Surg Oncol 33:956–960. https://doi.org/10.1016/j.ejso.2007.01.033
20. Selvaggi G, Novello S, Torri V, Leonardo E, De Giuli P, Borasio P et al (2004) Epidermal growth factor receptor overexpression correlates with a poor prognosis in completely resected non-small-cell lung cancer. Ann Oncol 15:28–32
21. Grassi ML, Palma CS, Thome CH, Lanfredi GP, Poersch A, Faca VM (2017) Proteomic analysis of ovarian cancer cells during epithelial-mesenchymal transition (EMT) induced by epidermal growth factor (EGF) reveals mechanisms of cell cycle control. J Proteomics 151:2–11
22. Shanmugapriya K, Kim H, Kang HW (2020) Epidermal growth factor receptor conjugated fucoidan/alginates loaded hydrogel for activating EGFR/AKT signaling pathways in colon cancer cells during targeted photodynamic therapy. Int J Biol Macromol 158:1163–1174
23. Rimassa L, Bozzarelli S, Pietrantonio F, Cordio S, Lonardi S, Toppo L et al (2019) Phase II Study of Tivantinib and Cetuximab in Patients With KRAS Wild-type Metastatic Colorectal Cancer With Acquired Resistance to EGFR Inhibitors and Emergence of MET Overexpression: Lesson Learned for Future Trials With EGFR/MET Dual Inhibition. Clin Colorectal Cancer 18:125–132
24. Mosmann T (1983) Rapid colorimetric assay for cellular growth and survival: application to proliferation and cytotoxicity assays. J Immunol Methods 65:55–63
25. Liu F, Liu D, Yang Y, Zhao S (2013) Effect of autophagy inhibition on chemotherapy-induced apoptosis in A549 lung cancer cells. Oncol Lett 5:1261–1265
26. Vermes I, Haanen C, Steffens-Nakken H, Reutelingsperger C (1995) A novel assay for apoptosis. Flow cytometric detection of phosphatidylserine expression on early apoptotic cells using fluorescein labelled Annexin V. J Immunol Methods 184:39–51
27. MacLachlan TK, Sang N, Giordano A (1995) Cyclins, cyclin-dependent kinases and cdk inhibitors: implications in cell cycle control and cancer. Crit Rev Eukaryot Gene Expr 5:127–156

28. Amin KM, Syam YM, Anwar MM, Ali HI, Abdel-Ghani TM, Serry AM (2018) Synthesis and molecular docking study of new benzofuran and furo[3,2-g]chromone-based cytotoxic agents against breast cancer and p38alpha MAP kinase inhibitors. Bioorg Chem 76:487–500
29. Zhu L, Hao J, Cheng M, Zhang C, Huo C, Liu Y et al (2018) Hyperglycemia-induced Bcl-2/Bax-mediated apoptosis of Schwann cells via mTORC1/S6K1 inhibition in diabetic peripheral neuropathy. Exp Cell Res 367:186–195
30. Karpova Y, Wu C, Divan A, McDonnell ME, Hewlett E, Makhov P et al (2019) Non-NAD-like PARP-1 inhibitors in prostate cancer treatment. Biochem Pharmacol 167:149–162
31. Vulpetti A, Bosotti R (2004) Sequence and structural analysis of kinase ATP pocket residues. Farmaco 59:759–765

Scheme

Scheme 1, 2 and 3 is available in supplementary section.

Figures

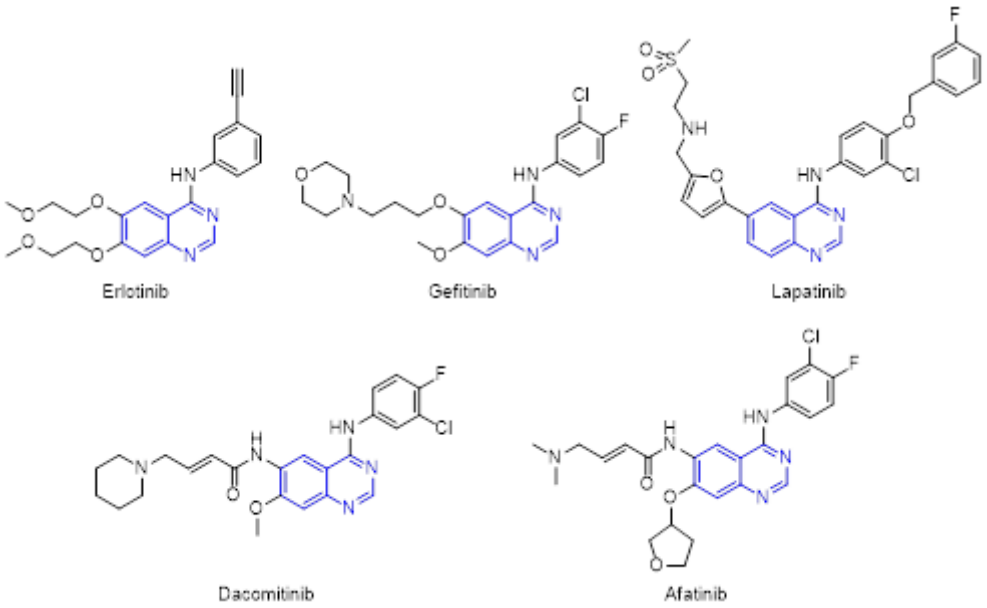

Figure 1

4-Anilinoquinazoline-based derivatives as EGFR-TK inhibitors

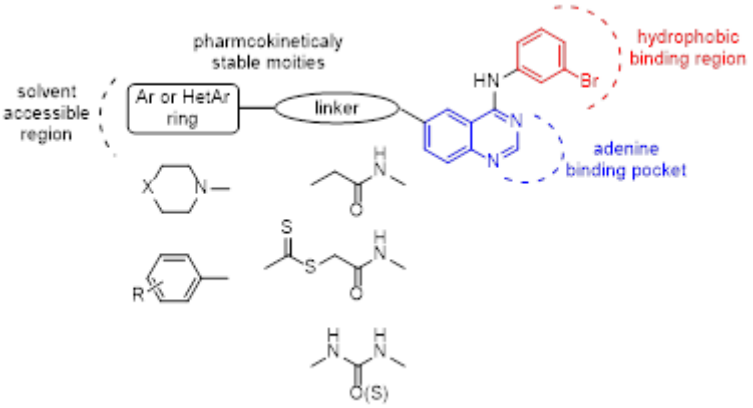

Figure 2

Diagram describes the essential parts for EGFR inhibitors and the rational design of the target compounds

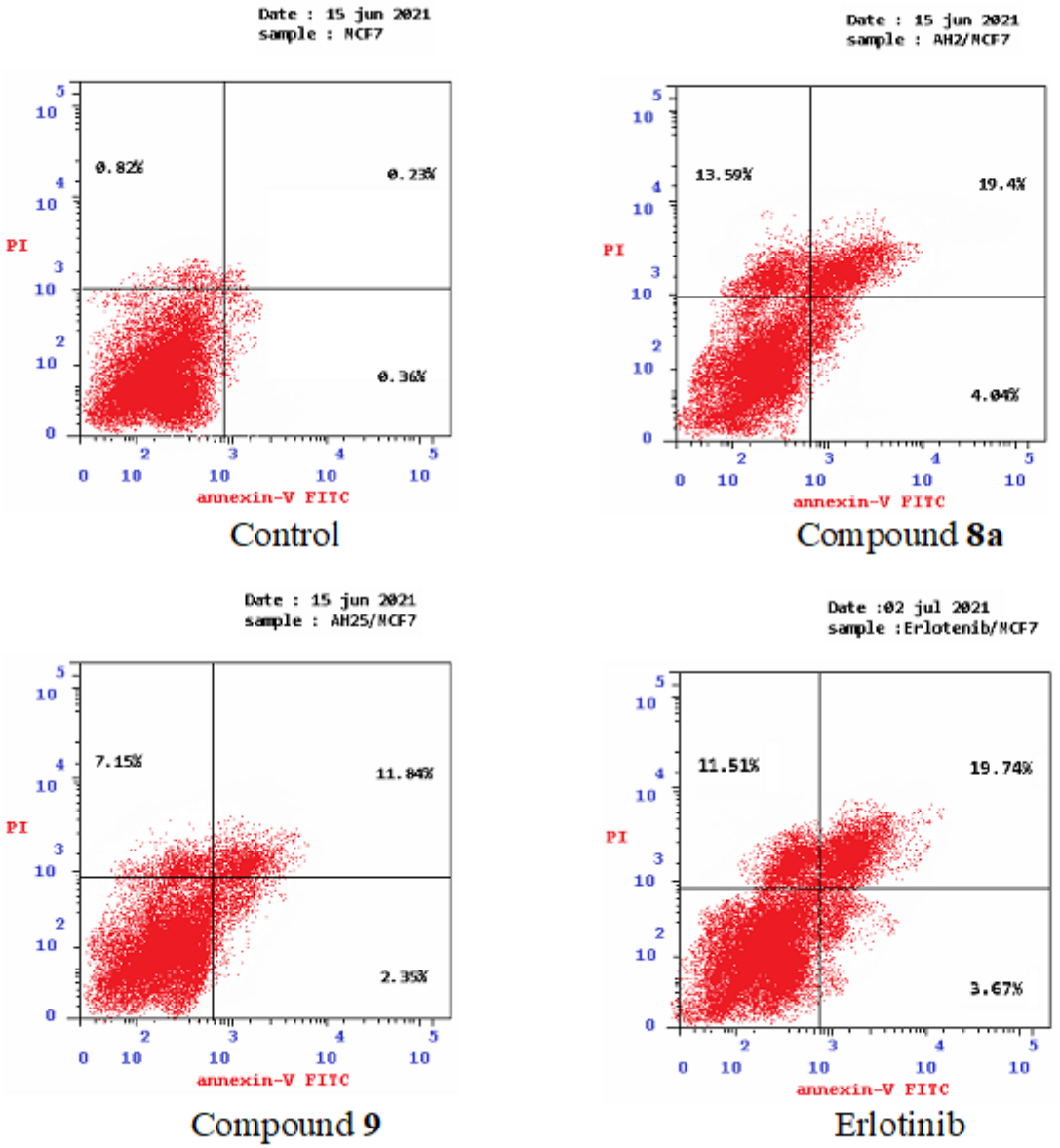

Figure 3

Activation of apoptosis caused by compounds **8a, 9** and Erlotinib in MCF-7 cells

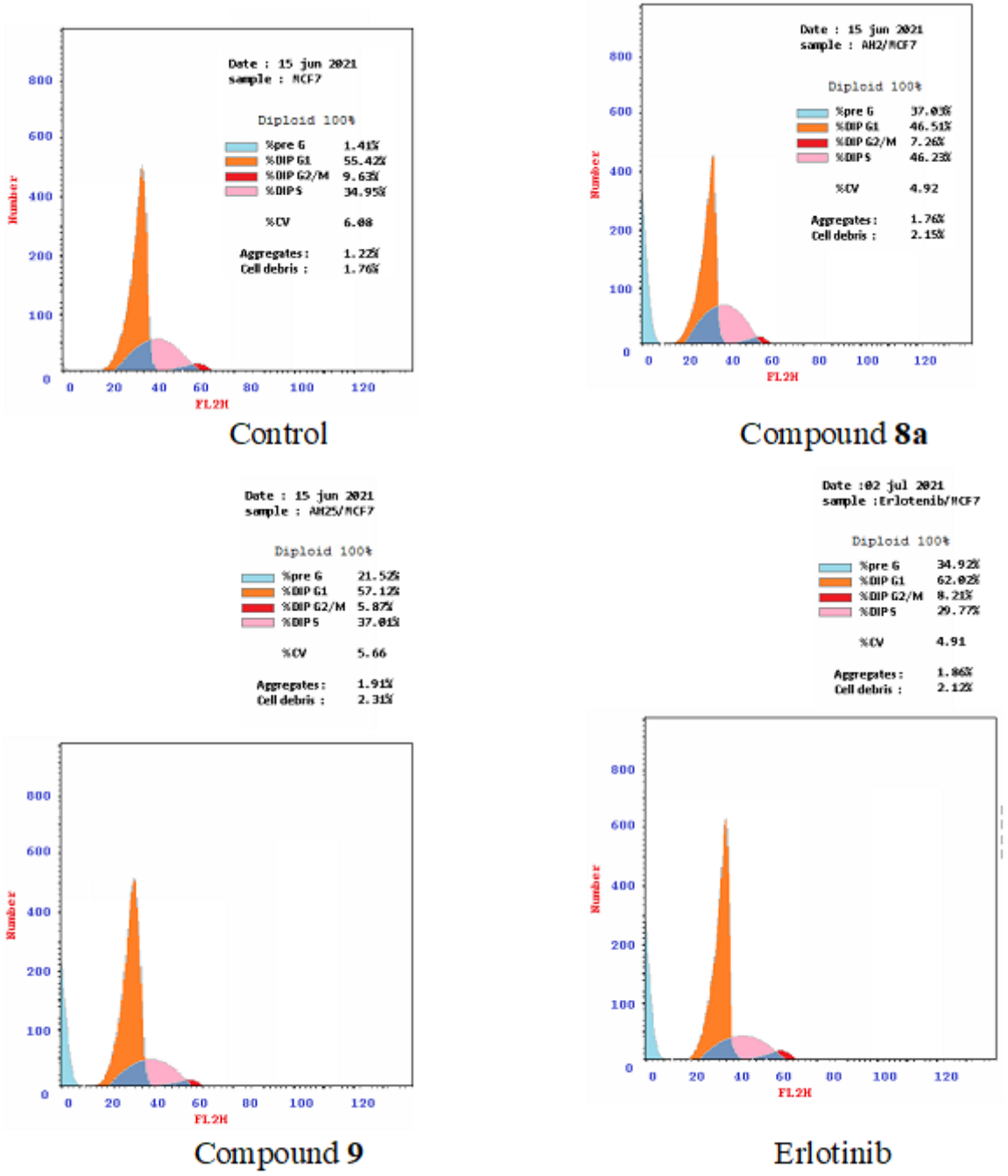

Figure 4

Analysis of cell cycle caused by compounds **8a, 9** and Erlotinib in MCF-7 cells

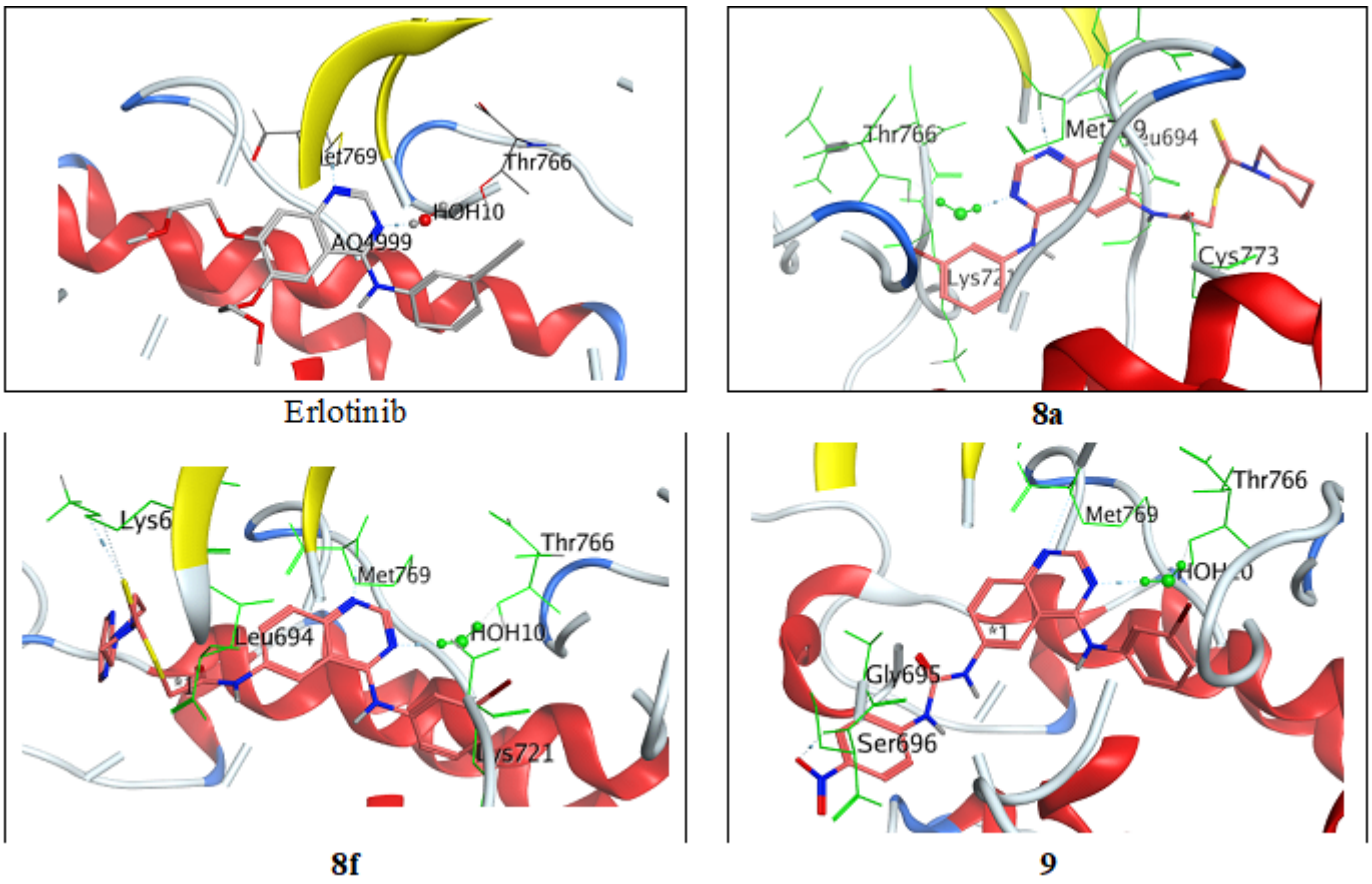

Figure 5

Docking of Erlotinib, **8a**, **8f** and **9** in the ATP binding site of EGFR TK (PDB code 1m17) in 3D view, exhibiting key hydrogen bonding (dotted lines) among N-1 of quinazoline hydrogen bonds with Met769 NH and the N-3 interacts with side chain of Thr766 through a water bridge

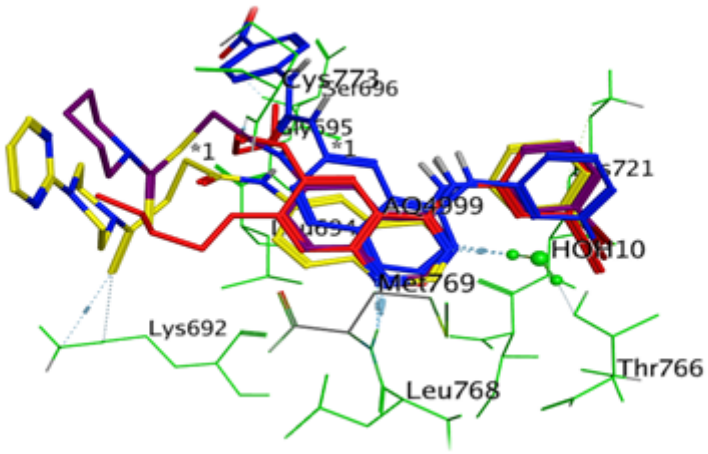

Figure 6

Visual representation of **8a** (violet), **8f** (yellow), **9** (blue), and Erlotinib (red) through the EGFR catalytic binding domain, where the cyan dotted line shows quinazoline N-1 hydrogen bonds with Met769 NH and

the N-3 interacts with the side chain of Thr766 through a water bridge

Supplementary Files

This is a list of supplementary files associated with this preprint. Click to download.

- Scheme01.png
- Scheme02.png
- Scheme03.png
- supportinginformationformedicinalchemistryresearch1.docx